Biochimica et Biophysica Acta 1832 (2013) 1591–1604

Contents lists available at SciVerse ScienceDirect

Biochimica et Biophysica Acta

journal homepage: www.elsevier.com/locate/bbadis

Hydrogen peroxide production regulates the mitochondrial function in insulin resistant muscle cells: Effect of catalase overexpression

Marina R. Barbosa [a,1], Igor H. Sampaio [a,1], Bruno G. Teodoro [a,g], Thais A. Sousa [a], Claudio C. Zoppi [c], André L. Queiroz [a], Madla A. Passos [a], Luciane C. Alberici [a,d,f,2], Felipe R. Teixeira [a], Adriana O. Manfiolli [a], Thiago M. Batista [c], Ana Paula Gameiro Cappelli [c], Rosana I. Reis [a], Danúbia Frasson [a], Isis C. Kettelhut [a], Lucas T. Parreiras-e-Silva [a], Claudio M. Costa-Neto [a], Everardo M. Carneiro [c], Rui Curi [e], Leonardo R. Silveira [a,b,f,*]

[a] Department of Biochemistry and Immunology, Faculty of Medicine of Ribeirão Preto, University of Sao Paulo (USP), Ribeirão Preto, SP, Brazil
[b] School of Physical Education and Sport of Ribeirão Preto, University of Sao Paulo, Ribeirão Preto, Brazil
[c] Department of Anatomy, Cell Biology and Physiology and Biophysics, Institute of Biology, State University of Campinas, Campinas, SP, Brazil
[d] Department of Physics and Chemistry, Faculty of Pharmaceutical Science of Ribeirão Preto, University of Sao Paulo, Ribeirão Preto, SP, Brazil
[e] Department of Physiology and Biophysics, Institute of Biomedical Sciences, University of São Paulo, São Paulo, Brazil
[f] Núcleo Pesquisas em Produtos Naturais e Sintéticos (NPPNS), Faculty of Pharmaceutical Sciences of Ribeirão Preto, University of São Paulo, Avenida do Café s/n, 14040-903, Ribeirão Preto, SP, Brazil
[g] Federal Institute of Education Science and Technology of São Paulo, Brazil

ARTICLE INFO

Article history:
Received 8 August 2012
Received in revised form 29 March 2013
Accepted 11 April 2013
Available online 2 May 2013

Keywords:
Mitochondria
Insulin resistance
Catalase and muscle cells

ABSTRACT

The mitochondrial redox state plays a central role in the link between mitochondrial overloading and insulin resistance. However, the mechanism by which the ROS induce insulin resistance in skeletal muscle cells is not completely understood. We examined the association between mitochondrial function and H_2O_2 production in insulin resistant cells. Our hypothesis is that the low mitochondrial oxygen consumption leads to elevated ROS production by a mechanism associated with reduced PGC1α transcription and low content of phosphorylated CREB. The cells were transfected with either the encoded sequence for catalase overexpression or the specific siRNA for catalase inhibition. After transfection, myotubes were incubated with palmitic acid (500 μM) and the insulin response, as well as mitochondrial function and fatty acid metabolism, was determined. The low mitochondrial oxygen consumption led to elevated ROS production by a mechanism associated with β-oxidation of fatty acids. Rotenone was observed to reduce the ratio of ROS production. The elevated H_2O_2 production markedly decreased the PGC1α transcription, an effect that was accompanied by a reduced phosphorylation of Akt and CREB. The catalase transfection prevented the reduction in the phosphorylated level of Akt and upregulated the levels of phosphorylated CREB. The mitochondrial function was elevated and H_2O_2 production reduced, thus increasing the insulin sensitivity. The catalase overexpression improved mitochondrial respiration protecting the cells from fatty acid-induced, insulin resistance. This effect indicates that control of hydrogen peroxide production regulates the mitochondrial respiration preventing the insulin resistance in skeletal muscle cells by a mechanism associated with CREB phosphorylation and β-oxidation of fatty acids.

Abbreviations: ROS, reactive oxygen species; DMEM, Dulbecco's Modified Eagle's Medium; PGM, prime growth medium (PGM); siRNA, Small interfering RNA; PGC1α, peroxisome proliferative activated receptor-γ (PPARγ) co-activator 1α; CREB, cAMP response element-binding; Akt, protein kinase B; KCl, potassium chloride; KH_2PO_4, potassium phosphate; $MgCl_2$, magnesium chloride; EGTA, ethylene glycol tetraacetic acid; FCCP, p-trifluoromethoxyphenylhydrazone; DTNB, 5, 5′-dithio-bis(2-nitrobenzoic acid); NaOH, sodium hydroxide; HCl, hydrochloric acid; PPARβ, peroxisome proliferative activated receptor-β; HRP, horseradish peroxidase; GAPDH, glyceraldehyde 3-phosphate dehydrogenase; Cu, Zn-SOD, Cu,Zn-superoxide dismutase; Mn-SOD, Mn-superoxide dismutase; CAT, catalase; GPX, glutathione peroxidase; ICAT, tricarboxylic acid cycle intermediates; Δψ, mitochondrial membrane potential (Δψ); NAC, N-acetylcysteine; ETF-QOR, transfer flavoprotein quinone oxidoreductase; CoQ, ubiquinone; UCP, uncoupling protein

* Corresponding author at: Department of Biochemistry and Immunology, Faculty of Medicine, University of São Paulo, Ribeirão Preto, Brazil. Tel.: +55 3602 4707, +55 16 3602 3213; fax: +55 16 3602 3213, +55 16 3602 4243.
E-mail address: lrs@icb.usp.br (L.R. Silveira).
[1] M.R. Barbosa and I.H.Sampaio contributed equally to this study.
[2] Tel.: +55 3602 4707; fax: +55 16 3602 4243.

0925-4439/$ – see front matter © 2013 Elsevier B.V. All rights reserved.
http://dx.doi.org/10.1016/j.bbadis.2013.04.029

1. Introduction

The resistance to insulin action in skeletal muscle is a major feature of type 2 diabetes. Although the number of studies in this area has grown exponentially, the mechanism responsible for the development of this pathology is not fully known. Randle and colleagues [1] were the first to propose that under high exposure to fatty acids, glucose utilization is substantially reduced in different tissues including skeletal muscle. The mechanism behind this biochemical process was known as the glucose–fatty acid cycle. Under such condition, the elevated content of acetyl-CoA inhibits pyruvate dehydrogenase complex (PDH) activity via activation of PDH kinase, the enzyme responsible for phosphorylation and inactivation of PDH. However, there is a consensus that a strong correlation exists between insulin resistance and high intracellular content of lipids [2–4].

In support of this lipotoxicity, studies in humans and rodents have demonstrated that elevated storage of triacylglycerol within skeletal muscle cells is accompanied by impaired insulin signaling [4–6]. The elevated content of triacylglycerol is also associated with changes in the intracellular redox state, which leads to low activity of the tricarboxylic acid cycle and reduced β-oxidation of fatty acids promoting insulin resistance [7,8]. Anderson et al. [9] observed that animals submitted to a high-fat diet exhibit elevated mitochondrial H_2O_2 production in isolated muscle fibers, suggesting an effect of fatty acids on mitochondrial ROS production. Paradoxically, physically active individuals were also demonstrated to exhibit an elevated content of intracellular triglyceride [10]. However, in contrast to insulin resistance, physically active individuals show elevated mitochondrial respiration and antioxidant capacity suggesting that a low mitochondrial activity associated with increased reactive oxygen species plays a key role for the establishment of insulin resistance in skeletal muscle cells [4,10,11]. However, the observations that ROS have a beneficial effect on insulin sensitivity when transiently increased, but are harmful when the increased concentration is sustained, as seen in response to chronic hyperglycaemia and dyslipidaemia [12,13], increase the suspicion that the primary cause of insulin resistance is determined by the mitochondrial function/ROS production ratio. In fact, in type II diabetes, the provision of nutrients in excess accompanied by low mitochondrial respiration rate has been described as the primary factor to induce insulin resistance in skeletal muscle cells. This condition supports the proposition that the mitochondrial redox state plays a central role in the link between mitochondrial overloading and insulin resistance [14]. However, the mechanism by which ROS induce insulin resistance in skeletal muscle cells is not completely understood. Given the important role of intracellular redox state and mitochondrial function affecting insulin response in skeletal muscle cells, we investigate how the elevated ROS production induced by palmitic acid treatment impairs the mitochondrial function and insulin response in skeletal muscle cells.

2. Methods

2.1. Isolation and culture of muscle cells

The procedures of cell isolation were previously approved by the Institutional Ethical Commit for use of laboratory animals from the University of São Paulo — Campus of Ribeirão Preto (Approval No. 092/2010). After sodium pentobarbital anaesthesia (40mg kg^{-1}), male Wistar rats weighing 50–60 g were killed by CO_2 inhalation. The soleus, gastrocnemius and quadriceps muscles were quickly isolated in Dulbecco's phosphate buffered saline (DPBS) medium containing glucose (1%) and penicillin (1%). The muscle tissue was minced and digested in Dulbecco's Modified Eagle's Medium (DMEM) containing collagenase II (1.5%), trypsin (2.5%), DNAse (0.1%) and penicillin (1%) at 37 °C for 30 min. The trypsin was neutralized with prime growth medium (PGM) (15 mL) containing horse serum (10%), fetal bovine serum (FBS) (10%), L-glutamine (2 mM) and penicillin (1%). The medium was centrifuged (4000 rpm) at 4 °C for 20 min and the supernatant discarded. The PGM (20 mL) was added and cell suspension filtered. The cells were placed in 6-well dishes covered with matrigel (0.1%) until they reach their mature stage (5–6 days) at a density of 250,000 cells/well [15].

2.2. Transfection

The plasmid containing the encoded sequence for catalase expression (pcDNA3) was amplified in bacteria (*E. coli* Top10, Invitrogen, Karlsruhe, Germany). When cells reached 40–60% confluence, they were washed and the culture medium changed for Opti-MEM® (Life Technology). The plasmid (1.6 μg) and Lipofectamine™2000 (Life Technology) were mixed in Opti-MEM® to form plasmid:Lipofectamine (1:4) complex and incubated for 20 min at room temperature. The complex was added to cell culture 48 h before differentiation (~60% confluence) and maintained at 37 °C with 5% CO_2 for 5 h. The cells were washed with DPBS and PGM medium added. As internal control, the cells were transfected with the empty pcDNA3 vector. At periods of 24, 48 and 72 h after the differentiation process, the content of catalase was determined by western blotting analysis.

2.3. siRNA transfection

The cells were transfected with specific siRNA oligos for catalase (SASI_RN02_0026086), Akt (SASI_RN01_00063656), PGC1α (SASI_RN01_00057042) and Creb (SASI_RN01_00042004 (sequence 1)/ SASI_RN01_00042680 (sequence 2) obtained from Sigma-Aldrich. The muscle cells were seeded in twelve-well plates at 8×10^4 cells/well. At 48 h before differentiation, the cell media were changed to antibiotic-free growth media (800 μL). The specific siRNA oligonucleotides (120 pmol — 20 nM/well) and Lipofectamine™2000 (Life Technology, USA) (6 μL/well) were added to antibiotic-free growth media (200 μL) at the beginning of differentiation process. This mixture was added to the cell dishes, and maintained at 37 °C with 5% CO_2 for 5 h. The cells were washed with DPBS and DMEM containing horse serum (10%) was added. At periods of 24 and 72 h after differentiation, the content of catalase was determined by western blotting analysis. The analyses of Creb and Akt were performed 24 h after the differentiation process.

2.4. Cell viability assay

After differentiation, the cells were exposed to increasing concentrations of palmitic acid (0, 100, 200, 500, 750 and 1250 μM) for 24 h. The cell viability was determined in a Neubauer-chamber utilizing trypan blue (4%).

2.5. Treatment of muscle cells with palmitic acid

After differentiation, the myotubes were incubated in DMEM medium containing palmitate (500 μM) for 24, 48 and 72 h. Briefly, a 100 mM stock solution of palmitc acid (Sigma, P5585) was prepared in ethanol. The stock of palmitic acid (100 mM) was diluted 200× (500 μM) in DMEM containing albumin (1%). This solution was lightly shaken at 40 °C for 20 min before being filtered through a 20 micrometer membrane [16].

2.6. Determination of ROS production

The cells were maintained at 37 °C in PBS containing either glucose (5.6 mM), fluorescent Amplex ultra-red (50 μM) or horseradish peroxidase (HRP) (0.1 U/mL) for 60 min. The medium was collected and fluorescence intensity determined at 568 nm excitation and 581 nm emissions. The cells were treated with either carnitine palmitoyltransferase-1 (CPT-1) inhibitor etomoxir (50 μM) or N-acetylcysteine (NAC) (10 mM). The antioxidants glutathione (GCH) plus glutathione peroxidase were utilized as a negative control.

2.7. The palmitic acid-induced reactive oxygen species production

After 24 h of incubation with palmitic acid (500 μM), the cells (7.5×10^5) were suspended in medium containing sacarose (125 mM), KCl (65 mM), KH_2PO_4 (2 mM), $MgCl_2$ (1 mM) and EGTA (0.1 mM). The pH was set at 7.33 and temperature kept at 36 °C. The cells were permeabilized with digitonin (3.5 μg/mL) and the experiments performed under respiratory state 4 by addition of oligomycin (2 μg/mL) [9]. The fluorescent amplex ultra-red (5 μM) and HRP (0.1 U/mL) were added to the cuvette (1 cm) equipped with a magnetic stirring system. The experiments were initiated by addition of malate (2 μM) plus glutamate (5 μM) followed by addition of succinate (12 μM). Rotenone (1 μM) was added to the medium as an inhibitor of complex I. The assay was performed during 30 min, after which the cells were removed for protein determination.

2.8. Citrate synthase activity

The citrate synthase activity was determined by spectrophotometric analysis using a kinetic assay based on the property of DTNB (Ellman reagent) to react with CoA-SH group (SH) [17].

2.9. Oxygen consumption

The cells were incubated in DMEM medium containing trypsin (0.25%) for 10 min at 37 °C. The cells were centrifuged at 15,000 *g* and suspended in DPBS (100 μL) before being added to the cuvette (1 mL) containing DPBS with pH set at pH 7.3 and temperature at 28 °C. Oligomycin (2 μg/mL) and p-trifluoromethoxyphenylhydrazone (2 μM) (FCCP) were added as ATP synthase inhibitor and mitochondrial uncoupling agent, respectively [18]. The oxygen consumption was monitored by Clark-type oxygen electrode (Hansatech, oxytherm electrode, UK).

2.10. Determination of glucose uptake

After a 4–5 h period in serum-free medium containing glucose (2 mM), the cells were incubated at 37 °C in DPBS (1 mL) containing glucose (5.6 mM), insulin (10,000 μU/mL) and 2-deoxy-[2,6^{3}H]-glucose (0.1 μCi/mL). After 30 min, the cells were washed in DPBS and lysed in NaOH (0.1 N) [19]. In an independent experiment, etomoxir (50 μM) was added to cell medium 60 min before the end of the experiments.

2.11. Glucose oxidation

After a 4–5 h period in serum-free medium containing glucose (2 mM), the cells were incubated for 60 min at 37 °C in Krebs Ringer solution in the presence of glucose (5.6 mM) and U-^{14}C-glucose (0.2 μCi/mL). The assay was acidified with HCl (5N) and the $^{14}CO_2$ produced was quantified using phenylethylamine [20].

2.12. Determination of fatty acid oxidation

After a 4–5 h period in serum-free medium containing glucose (2 mM), the cells were incubated for 60 min at 37 °C in Krebs Ringer solution in the presence of [U-^{14}C]-palmitic acid (0.2 μCi/mL) [20]. The fatty acid oxidation was determined by measuring $^{14}CO_2$ production. The buffer was acidified with 0.25 mL of H_2SO_4 (5N).

2.13. Western blotting analysis

Aliquots of cell lysate (15–25 μg of protein) were separated by SDS-PAGE gel and transferred to nitrocellulose membrane. After being blocked with milk (5%), the membrane was incubated overnight at 4 °C with appropriate dilutions of primary antibodies, including anti-catalase (Sigma-aldrich), p-Akt, t-Akt, p-CREB, t-CREB, β-actin (Cell Signaling Technology). After washing in TBST (3 × 10 min), membranes were incubated with the appropriate secondary antibody conjugated with HRP for 120 min at room temperature. Antibody binding was detected by enhanced SuperSignal® West Pico Chemiluminescent Substrate (PIERCE, IL, USA), as described by the manufacturer. Blots were scanned (Epson expression 1600) and the densitometry of protein bands was determined by pixel intensity using Scion Image software (Scion Corporation, MD, USA). The β-actin blotting was used as an internal control.

2.14. Analysis of mRNA expression

Total RNA was isolated using the TRIzol reagent (Invitrogen, USA). For real-time PCR analysis, RNA was reverse transcribed using the Power SYBER green master mix (Applied Biosystems, FosterCity, CA, USA). cDNA synthesis kit and used in quantitative PCR reactions containing SYBR-green fluorescent dye (ABI). Relative expression of mRNAs was determined after normalization with GAPDH using the $^{\Delta\Delta}$Ct method [21]. Quantitative PCR was performed using Applied Biosystems StepOne® Real-Time PCR System (Applied Biosystems, FosterCity, USA). Primers for PGC1α, catalase, Creb, PPAR, Cu,Zn-SOD, Mn-SOD, GPX, PPARβ were designed as described in Table 1.

2.15. Tricarboxylic acid cycle intermediates (ICAT)

Briefly, the cells were scraped off in perchloric acid (0.5 M) containing EDTA (1 mM) and neutralized with $KHCO_3$ (2.2 M). The concentrations of the ICAT were determined using a standard curve containing different concentration of citrate, malate, oxaloacetate and isocitrate. The fluorimetric enzymatic assays were performed as previously described [22].

2.16. Statistical analysis

Results were expressed as mean ± standard error of mean (S.E.M) and analyzed by Student *t* test and one-way/two-way ANOVA followed by post-Kruskal–Wallis, $p < 0.05$.

3. Results

3.1. Catalase overexpression

The catalase transfection was initiated 48 h before differentiation. Its content was observed to increase ~3.8, 3.9 and 4.2-fold at periods of 24, 48 and 72h, respectively after transfection (Fig. 1A). As a control experiment, the empty plasmid had no effect on catalase content (Fig. 1B). In contrast, when the cells were transfected with specific siRNA targeting catalase at 48 h before differentiation, the enzyme expression was depressed by ~60% during the period of 48 h after cell transfection as compared to control (Fig. 1C).

3.2. Effect of palmitic acid on cell viability and on oxygen consumption

Before starting the experiments we exposed muscle cells to different concentrations of palmitic acid including 0, 100, 200, 500, 750 and 1250 μM. The cell viability was not changed compared to control, as demonstrated in Fig. 2, panel A. However, at concentrations above 500 μM the rate of mitochondrial oxygen consumption was markedly reduced indicating that at this concentration of palmitc acid the mechanism of insulin resistance might be stimulated through reduced mitochondrial respiration (Fig. 2B). After 24 h of palmitic acid treatment at concentrations of 500 and 750 μM, the hydrogen peroxide production was markedly elevated compared to control. This effect was abolished when palmitic acid treatment was combined with glutathione (GSH) plus glutathione peroxidase (GPX) (Fig. 2C). Similarly, the Akt phosphorylation level was substantially reduced after exposure of the cells to 500 or 750 μM of palmitic acid during the period of 24 h

Table 1
Sense and antisense sequences of the primers used in the real time RT-PCR assays. PGC1α; peroxisome proliferative activated receptor-β co-activator 1α; PPARβ, peroxisome proliferative activated receptor-β; Cu,Zn-SOD, Cu,Zn-superoxide dismutase1; Mn-SOD, Mn-superoxide dismutase2; CAT, catalase; GPX, glutathione peroxidase; GAPDH, glyceraldehyde 3-phosphate dehydrogenase; β-actin.

Gene	Sense	Antisense	Size (bp)
PGC1α	5′CAAGCCAAACCAACAACTTTATCTCT3′	5′CACACTTAAGGTTCGCTCAATAGTC3′	102
Cu,Zn-SOD	5′CCAGCGGATGAAGAGAGG3′	5′CCAATCACACCACAAGCC3′	230
Mn-SOD	5′GACCTGCCTTACGACTATG3′	5′TACTTCTCCTCGGTGACG3′	119
GPX	5′GTTCGGACATCAGGAGAATGG3′	5′GGGTTCGATGTCGATGGTGC3′	331
CAT	5′ATTGCCGTCCGATTCTCC3′	5′CCAGTTACCATCTTCAGTGTAG3′	105
GAPDH	5′TGCCATCACTGCCACTC3′	5′CTGCTTCACCACCTTCTTG3′	256
Creb1	5′ACCCCGATTTACCAAACTAGC3′	5′CTTGGTTGCTGGGCACTAGA3′	205
PPARβ	5′GGCCTTCTCCAAGCACATCT3′	5′CATGCACGCTGATCTCGTTG3′	206
β-actin	5′CACTTTCTACAATGAGCTGCG3′	5′CTGGATGGCTACGTACATGG3′	148

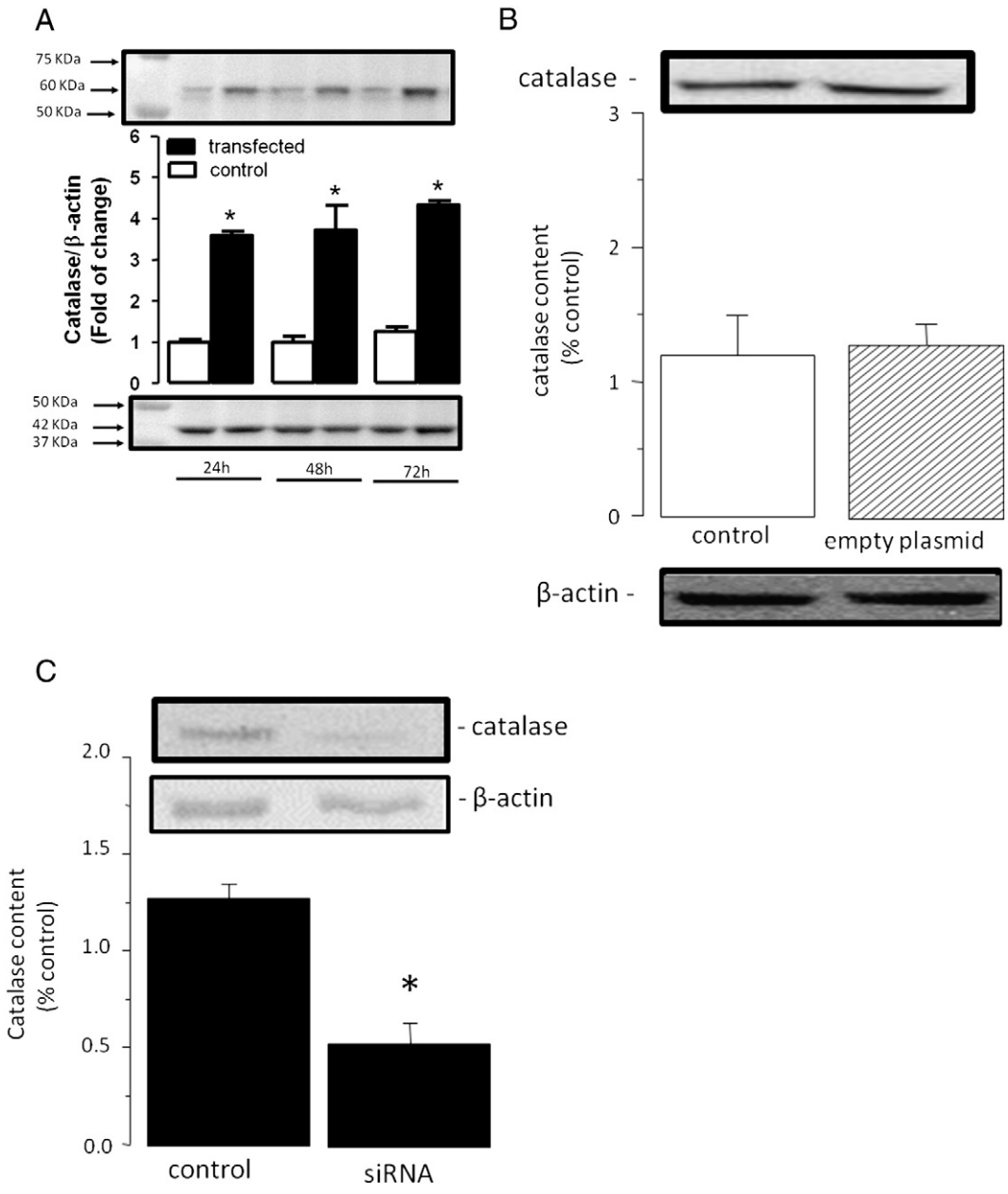

Fig. 1. Content of catalase after transfection: A) The catalase content determined by western blotting after transfection at time 24, 48 and 72 h after differentiation. *$p < 0.05$ compared to control ($n = 6$); B) Effect of empty plasmid on catalase content at 48 h after transfection ($n = 3$). C) Inhibition of catalase expression using siRNA. The catalase content was determined by western blotting at 48 h after cell transfection, *$p < 0.05$ ($n = 6$). β-actin was used as internal control.

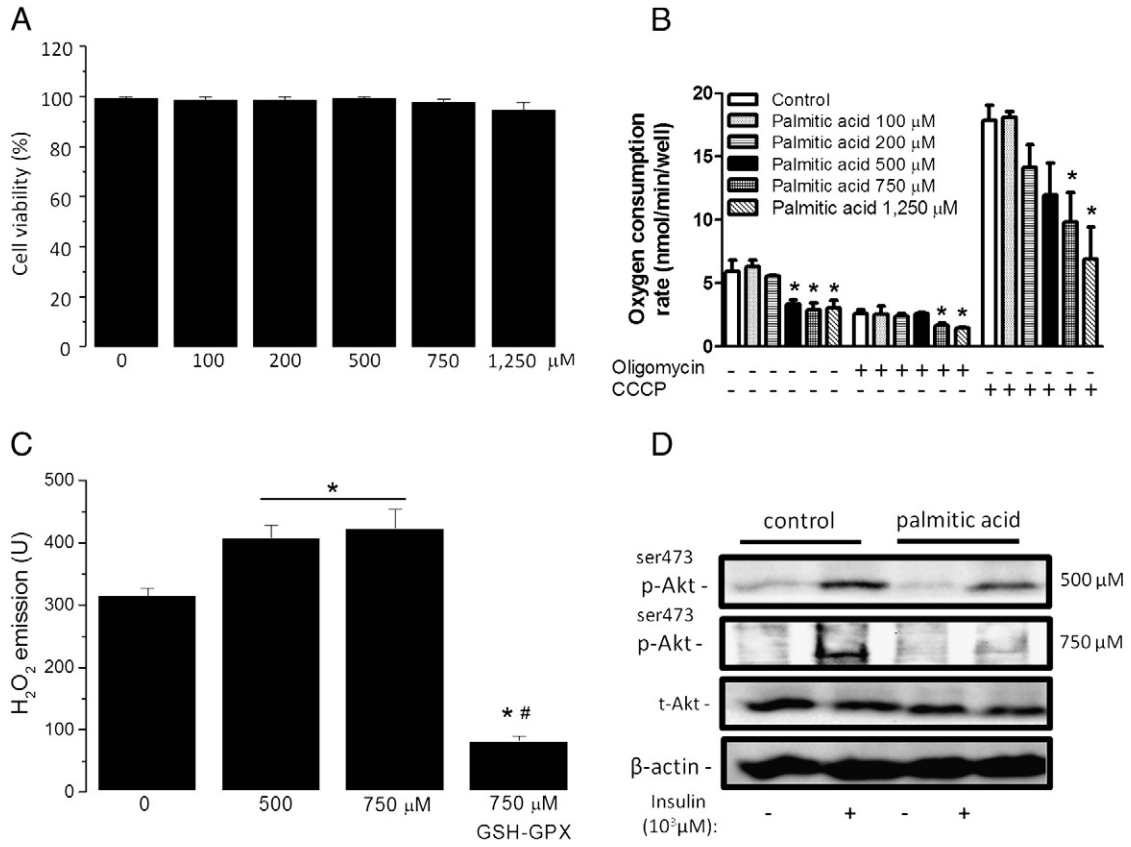

Fig. 2. Effect of different concentrations of palmitic acid on cell viability, on oxygen consumption and H_2O_2 production. A) The cells were incubated in the presence of different concentrations of palmitic acid including 0, 100, 200, 500, 750 and 1250 μM during 24 h. The cell viability was determined in a Neubauer-chamber utilizing trypan blue (4%). B) The rate of oxygen consumption was obtained from control and palmitic acid treated cells after the period of 24 h treatment. The ATP synthase inhibitor oligomycin (1.5 μg/mL) and the mitochondrial uncoupling carbonyl cyanide p-trifluoromethoxy-phenylhydrazone (FCCP) (2 μM) were added as negative and positive controls, respectively. *$p < 0.05$ compared to its respective control; The effect of palmitic acid on hydrogen peroxide production in skeletal muscle cells: C) the results are the mean ± SEM of extracellular hydrogen peroxide content determined by amplex ultra-red fluorescent probe at the time of 24 h of palmitic acid treatment. *$p < 0.05$ compared to control; #$p < 0.05$ compared to the cells treated with palmitic acid 500 and 750 μM ($n = 6$); D) effect of two different concentrations of palmitic acid (500 and 750 μM) on Akt phosphorylation level determined by western blotting analysis in cultured muscle cells after 24 h of palmitic acid treatment. The cells were incubated in serum-free medium containing either glucose (5.6 mM) or glucose plus insulin (10,000 μU/mL) for 30 min ($n = 3$).

(Fig. 2D). These findings are, therefore, indicating that the elevated rate of hydrogen peroxide combined with reduced mitochondrial respiration contribute to a low insulin response in skeletal muscle cells.

3.3. Effect of palmitic acid on intracellular antioxidant system

The exposure of cells to palmitic acid (500 μM) did not reduce the intracellular catalase content after differentiation periods (Fig. 3A). However, we observed a marked reduction on transcription of enzymatic antioxidant system including catalase, superoxide dismutase (Cu,Zn-SOD), superoxide dismutase (Mn-SOD) and gluthione peroxidase (GPX). This effect was prevented by catalase overexpression (Fig. 3B). In addition, the intracellular GSH/GSSG ratio was marked reduced after palmitic acid treatment for 48 h (Fig. 3C). This effect was accompanied by elevated rate of hydrogen peroxide production (Fig. 3D).

3.4. Catalase overexpression protected the cells from hydrogen peroxide

The hydrogen peroxide was elevated after palmitic acid treatment by ~31, 36, and 20% compared to control, at the periods of 24, 48 and 72 h, respectively. This effect was abolished when palmitic acid treatment was combined with catalase overexpression at 24, 48 and 72 h. In addition, the catalase overexpression in control cells was observed to markedly depress the hydrogen peroxide release by 31, 30 and 33% at the periods of 24, 48 and 72 h, respectively (Fig. 4A). As a negative control, the fatty acid treated cells were also incubated with NAC. The NAC compound increases the intracellular glutathione (GSH) content raising the antioxidant capacity of the cells. Under such condition, we observed a marked reduction in hydrogen peroxide production as compared to fatty acid treated cells by 68.3, 61.3 and 67.5% at 24, 48 and 72 h, respectively (Fig. 4B). In order to investigate the association of the β-oxidation of fatty acids and the mitochondrial ROS production, we treated the cells with etomoxir, a well known carnitine palmitoyl transferase inhibitor. After etomoxir treatment, the hydrogen peroxide release was substantially attenuated by 14.2, 22.2 and 19.6%, at the periods of 24, 48 and 72 h, respectively (Fig. 4C). It is important to note that in permeabilized cells respirating in the presence of mitochondrial complex I substrates malate and glutamate, there was an increase in the hydrogen peroxide production only in the control cell. However, the addition of mitochondrial complex II substrate succinate markedly increased the rate of hydrogen peroxide production in palmitic acid treated cells. To investigate the contribution of mitochondrial complex I on the rate of H_2O_2 production, we observed in fatty acid treated cells that rotenone, an inhibitor of complex I, decreased the rate of hydrogen peroxide production by ~7% (Fig. 4D).

3.5. Effect of palmitic acid and catalase transfection on glucose uptake and Akt phosphorylation

The glucose uptake induced by insulin in control cells was elevated by ~110, 114 and 67% at periods of 24, 48 and 72 h, respectively.

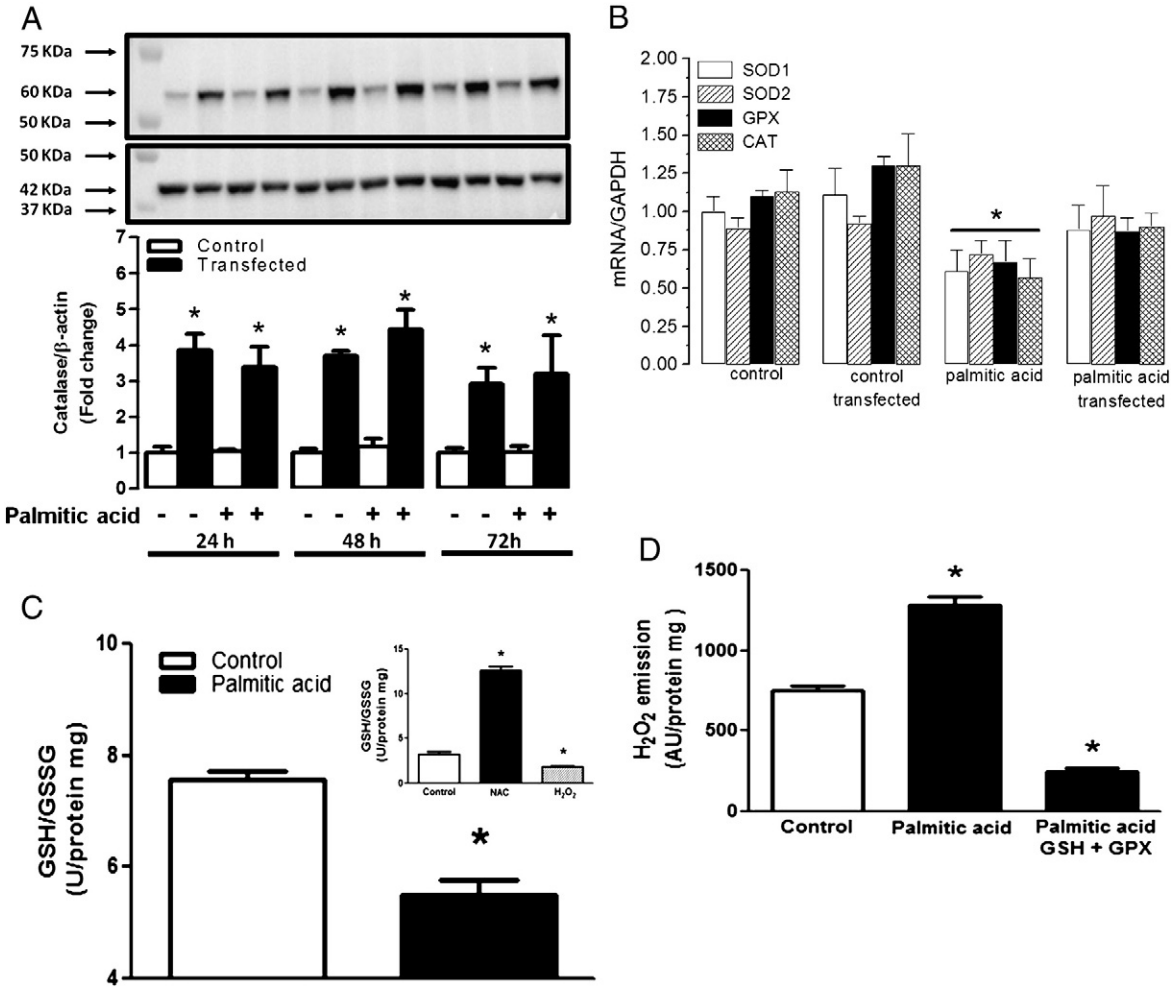

Fig. 3. Content of catalase during palmitic acid treatment. A) Densitometric analyses of catalase and β-actin content determined by western blotting at the periods of 24, 48 and 72 h in cultured muscle cells. The results are presented as the mean ± SEM *$p < 0.05$ compared to its control ($n = 8$ experiments); B) transcription of enzymatic antioxidant system after 24 h of palmitic acid treatment. The values are mean ± SEM of mRNA from Cu,Zn-superoxide dismutase (SOD1), Mn-superoxide dismutase (SOD2), catalase (CAT) and glutathione peroxidase (GPX). *$p < 0.05$ compared to control ($n = 7$); C) effect of palmitic acid treatment on intracellular GSH/GSSG ratio. The insert shows a control experiments using positive (NAC, 10 mM) and negative (H_2O_2, 0.3 mM) control, *$p < 0.05$ compared to control ($n = 8$ experiments); D) The hydrogen peroxide production in control, palmitic acid treated cells and palmitic acid treated cells plus GSH (0.05 mM)/glutathione peroxidase (0.3 U/mL), *$p < 0.05$ compared to control ($n = 5$).

Similarly, insulin increased the glucose uptake in control cells after catalase transfection. On the other hand, in fatty acid treated cells the insulin increased the glucose uptake by only 37.5, 43 and 28% compared to controls without insulin at 24 and 48 and 72 h, respectively. However, the catalase overexpression improved the insulin response in fatty acid treated cells increasing the glucose uptake by 60, 49 and 35%, at the periods of 24, 48 and 72 h, respectively (Fig. 5A). In addition, the basal glucose uptake into the palmitic acid transfected cells was observed to increase compared to palmitic acid non-transfected cells at periods of 24 and 48 h. In the presence of insulin, glucose uptake was also reduced when catalase expression was suppressed by using specific siRNAs compared to controls without insulin (95 ± 33 vs. 122 ± 7, $p > 0.05$). The inhibition of catalase expression in control cells reduced glucose uptake induced by insulin, whereas in the palmitic acid treated cells this effect was observed with or without insulin (31 ± 11 vs. 35 ± 12) (Fig. 5B). The Akt phosphorylation induced by insulin in fatty acid treated cells was lower (22%) than that in control cells (172%). The overexpression of catalase was able to prevent the reduction of Akt phosphorylation in muscle cells treated with palmitic acid (226%) (Fig. 5C). Interestingly, the reduction on Akt phosphorylation level observed in palmitic acid treated cells in the presence of insulin was of ~29% compared to control. This palmitic acid effect was prevented by etomoxir, which was observed to increase the Akt phosphorylation level in the presence of insulin to the same level of control cells (Fig. 5D). This response was reflected in elevated insulin sensitivity as indicated by glucose uptake assay suggesting a strong association between the β-oxidation of fatty acid and the mechanism of insulin resistance in skeletal muscle cells (Fig. 5E).

3.6. Effect of palmitic acid and catalase transfection on mitochondrial biogenesis

The PGC1α transcription was reduced in fatty acid treated cells by 71.5% at 24 h. The overexpression of catalase prevented this effect, exhibiting a PGC1α mRNA level similar to the control (Fig. 6A). When the catalase expression was inhibited, both control and fatty acid treated cells exhibited a reduction in PGC1α transcription at 24 and 72 h (Fig. 6B). According to the above findings, the citrate synthase activity which is closely related to mitochondrial respiration was observed to decrease after fatty acid treatment by 42, 72, and 58%, at 24, 48 and 72 h, respectively. The catalase overexpression abolished this effect (Fig. 6C). In addition, the fatty acid treatment was also observed to reduce the ICAT including citrate, malate and oxaloacetate, whereas the catalase transfection attenuated this effect (Fig. 6D).

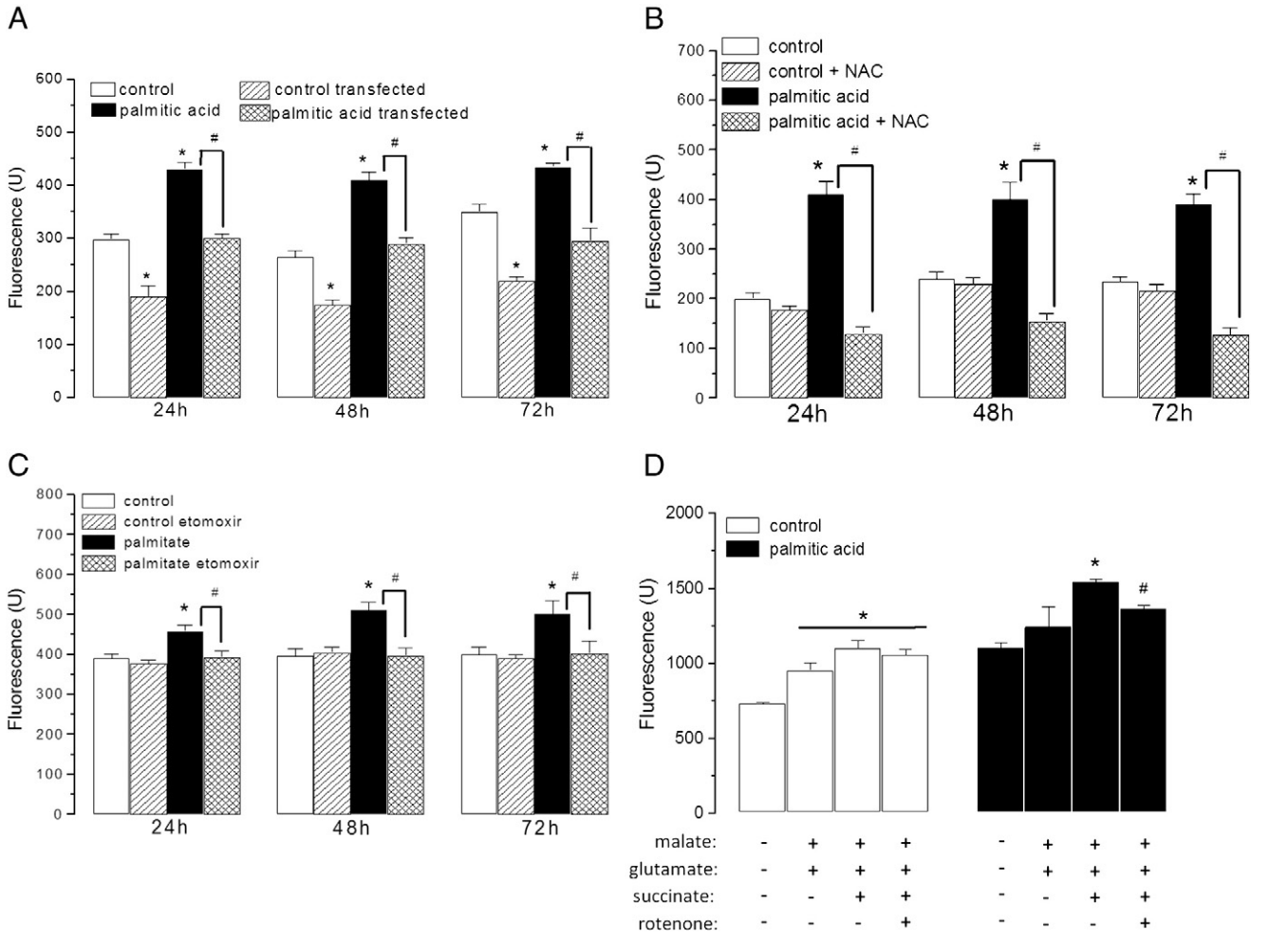

Fig. 4. The effect of palmitic acid on hydrogen peroxide production in skeletal muscle cells: A) the results are the mean ± SEM of extracellular hydrogen peroxide content determined by amplex ultra-red fluorescent probe at times of 24, 48 and 72 h of palmitic acid treatment. *p < 0.05 compared to control; #p < 0.05 compared to palmitic acid (n = 8–10); B) effect of N-acetylcysteine (NAC) on hydrogen peroxide production in palmitic acid treated cells at periods of 24, 48 and 72 h. *p < 0.05 compared to control (n = 6 experiments); #p < 0.05 compared to palmitic acid; C) effect of carnitine palmitoyl transferase inhibitor, etomoxir, on hydrogen peroxide production. The results are the mean ± SEM of hydrogen peroxide at periods of 24, 48 and 72 h after incubation with palmitic acid (500 μM) and/or etomoxir (50 μM). *p < 0.05 compared to control; #p < 0.05 compared to palmitic acid (n = 6); D) effect of palmitic acid treatment on hydrogen peroxide production determined by amplex ultra-red fluorescent probe in isolated muscle cells during 30 min. The experiments were performed on permeabilized cells suspended in DPBS buffer containing oligomycin (2 μg/mL). The fluorescent amplex ultra-red (5 μM) and HRP (0.1 U/L) was added to the medium and the experiments initiated by addition of malate (2 μM), glutamate (5 μM) and succinate (12 μM). In independent experiments, rotenone (1 μM) was added to the medium as inhibitor of complex I. *p < 0.05 compared to its control; #p < 0.05 compared to succinate bar (n = 5 experiments).

3.7. Catalase overexpression protected the fatty acid-associated declines in mitochondrial oxygen consumption

The oxygen consumption was reduced in fatty acid treated cells by 50, 73 and 84%, at 24, 48 and 72 h, respectively. The magnitude of oxygen consumption in fatty acid treated cells was lower at 48 h (7 nmol/min) and 72 h (4 nmol/min) than in the 24 h (14 nmol/min) period. In contrast, catalase overexpression prevented this effect exhibiting elevated oxygen consumption when the fatty acid treated cells were compared to the control. In the periods of 48 and 72 h, the oxygen consumption by the fatty acid treated cells overexpressing catalase was lower compared to the same group at 24 h. The insert shows that oxygen consumption was previously calibrated (Fig. 6E). The oxygen consumption was reduced after catalase siRNA knockdown in control cells at 24 h (~42%) and 72 h (~40%). Similarly, siRNA knockdown reduced oxygen consumption in fatty acid treated cells at 24 h (~50%) and 72 h (~50%) (Fig. 6F), indicating that elevated concentrations of hydrogen peroxide exert a negative effect on the mitochondrial biogenesis process and consequently on mitochondrial function. In fact, after inhibition of PGC1α transcription we observed a marked decrease in oxygen consumption, an effect that was reflected in a low Akt phosphorylation level, demonstrating that the impaired insulin response is associated with the reduced mitochondrial function in skeletal muscle cells (Fig. 7A, B and C).

3.8. Catalase overexpression improves the glucose and fatty acid metabolism in insulin resistant muscle cells

To determine whether protection from fatty acid-associated declines in mitochondrial function would result in improvement in glucose and fatty acid metabolism, we analyzed glucose metabolism and fatty acid oxidation. The fatty acid treated cells showed impaired metabolism, as reflected by a ~29% of reduction in $^{14}CO_2$ produced from U-^{14}C-glucose (Fig. 8A) and 41% of reduction from U-^{14}C-palmitic acid (Fig. 8B). This impairment was prevented with catalase overexpression (Fig. 8A, B). The palmitic acid oxidation was increased in transfected cells (~34%), whereas etomoxir reduced palmitic acid oxidation by 73% (Fig. 8B). However, it is important to note that we were not able to see any effect on PPAR-β transcription level (Fig. 8C), whereas the transcription of hydroxyacyl-coA-dehydrigenase (HACD) was markedly increased in palmitic acid treated cells.

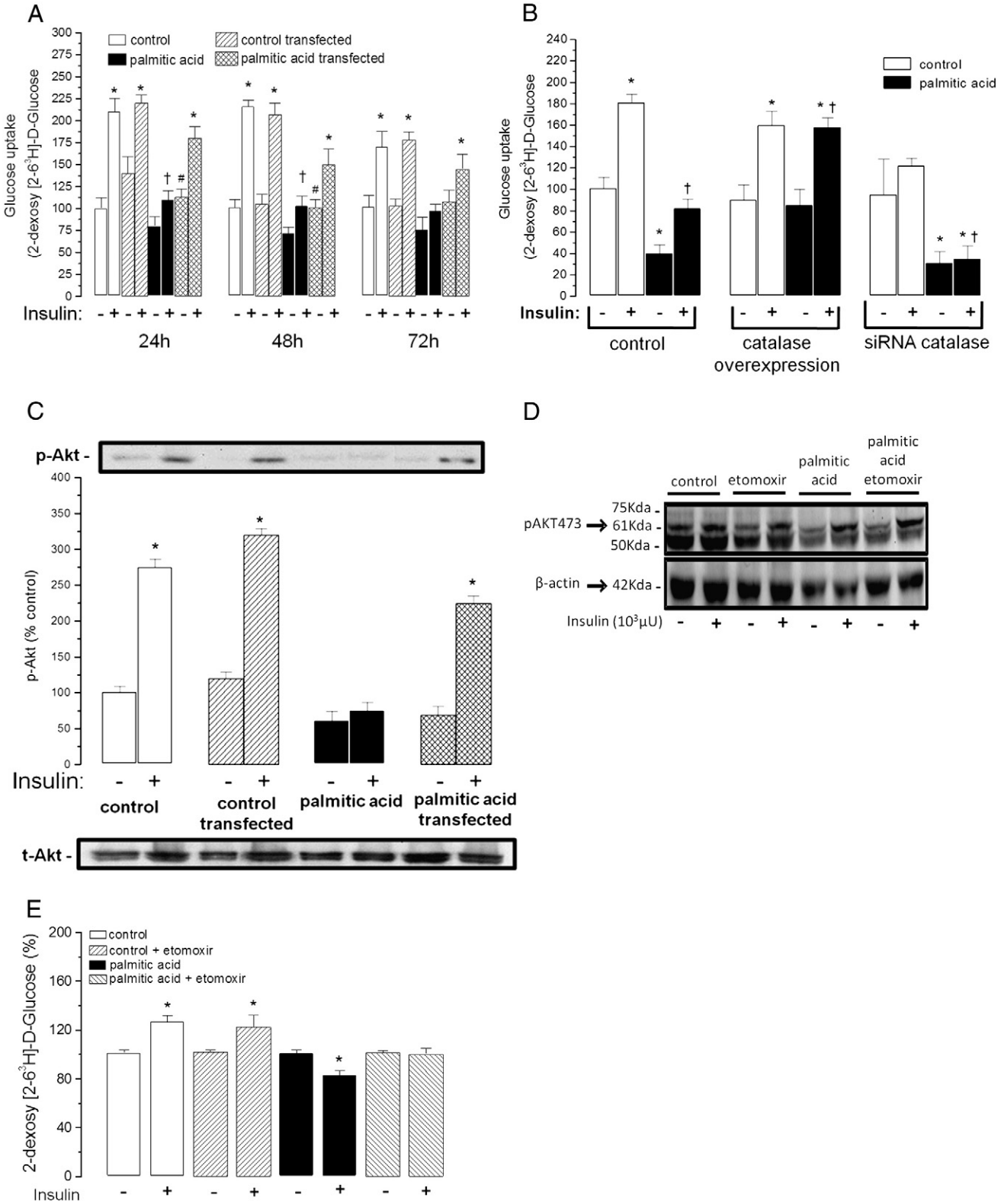

Fig. 5. Glucose uptake in skeletal muscle cells. A) Effect of palmitic acid treatment on muscle cells incubated in serum-free medium containing glucose, (5.0 mM), insulin (10,000 μU/mL) and 2-deoxy-[2,6^{3}H]-glucose (0.1 μCi/ml). After 30 min, the cells were washed twice in DPBS and then lysed in NaOH and radioactivity determined. *$p < 0.05$ compared to control, †$p < 0.05$ compared to palmitic acid without insulin ($n = 10–12$); #$p < 0.05$ compared to palmitic acid group without insulin. B) Glucose uptake in muscle cells after inhibition of catalase expression. The cells were transfected with pcDNA3 containing catalase encoding sequence or siRNA sequence for catalase and exposed to palmitic acid for 24 h. The uptake of 2-deoxy-[2,6^{3}H]-glucose (0.1 μCi/ml) at the presence or absence of insulin (10,000 μU/mL) was determined after 30 min. *$p < 0.05$ compared to control, †$p < 0.05$ compared to palmitic acid without insulin ($n = 6$) and C) Akt phosphorylation. The values are mean ± SEM from densitometric analyses of phosphorylated and total content of Akt as determined by western blotting in cultured muscle cells after 24 h of palmitic acid treatment. The cells were incubated in serum-free medium containing either glucose (5.6 mM) or glucose plus insulin (10,000 μU/mL) for 30 min. *$p < 0.05$ compared to control ($n = 6$ experiments); D) effect of etomoxir treatment on phosphorylated and total content of Akt as determined by western blotting in cultured muscle cells after 24 h of palmitic acid treatment ($n = 4$ experiments); E) effect of etomoxir treatment on glucose uptake in skeletal muscle cells, *$p < 0.05$ compared to its respective control without insulin ($n = 6$ experiments).

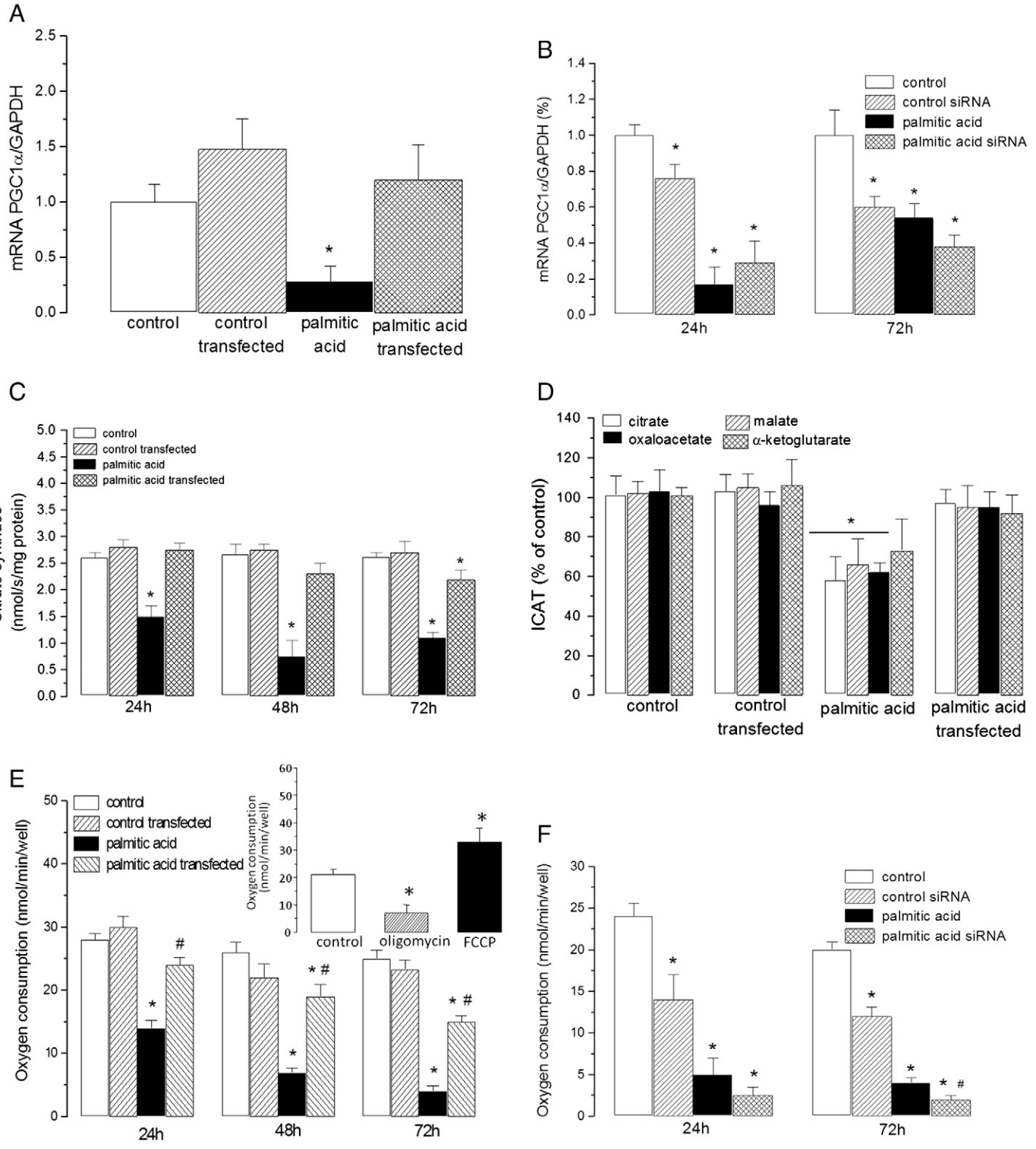

Fig. 6. Mitochondrial biogenesis and function. A) Transcription of PGC1-α in skeletal muscle cells after 24 h of palmitic acid treatment. *$p < 0.05$ compared to control ($n = 8–10$); B) mRNA levels of PGC1-α in skeletal muscle cells after catalase inhibition. The catalase transcription was inhibited using siRNA. *$p < 0.05$ compared to control ($n = 6$); C) citrate synthase activity. The values are the mean ± SEM of citrate synthase activity in skeletal muscle cells after 24, 48 and 72 h of palmitic acid treatment. *$p < 0.05$ compared to control ($n = 8$); D) Content of tricarboxylic acid cycle intermediates (ICAT) including citrate, malate, oxaloacetate and α-ketoglutarate. The values are the mean ± SEM of ICAT in skeletal muscle cells after 24 h of palmitic acid treatment. *$p < 0.05$ compared to control ($n = 5–8$); E) the rate of oxygen consumption by muscle cells. The oxygen consumption was measured in control, control transfected with catalase, palmitic acid treated cells and palmitic acid treated cells transfected with catalase at periods of 24, 48 and 72 h. The effect of catalase overexpression was observed in palmitic acid treated cells at periods of 24, 48 and 72 h. *$p < 0.05$ compared to control; #$p < 0.05$ compared to palmitic acid ($n = 6$). The insert exhibited in the figure. Panel A shows the calibration of oxygen consumption in isolated muscle cells. The ATP synthase inhibitor oligomycin (1.5 μg/mL) and the mitochondrial uncoupler carbonyl cyanide p-trifluoromethoxy-phenylhydrazone (FCCP) (2 μM) were added as negative and positive controls, respectively. *$p < 0.05$ compared to control; #$p < 0.05$ compared to palmitic acid ($n = 6$) and F) Oxygen consumption after inhibition of catalase expression. The catalase expression was inhibited using siRNA (20 nM) in control and palmitic acid treated cells at periods of 24 and 72 h. *$p < 0.05$ compared to control; #$p < 0.05$ compared to control transfected with catalase siRNA ($n = 5$).

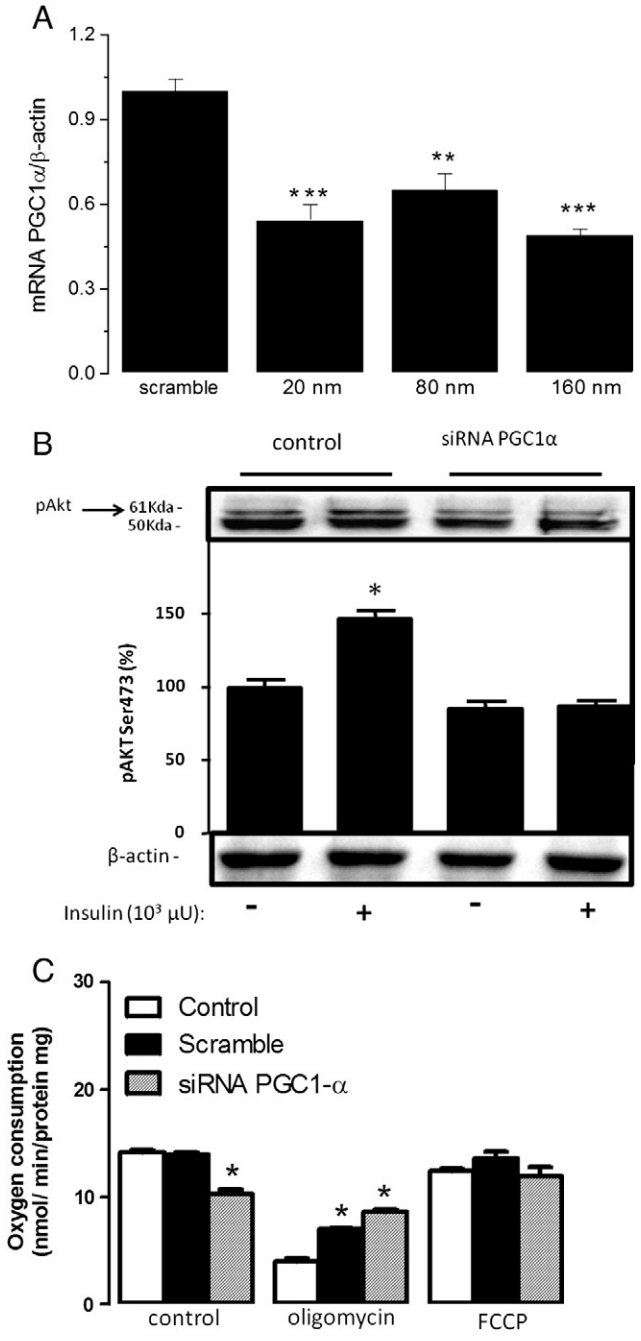

Fig. 7. Effect of PGC1α inhibition on oxygen consumption and insulin response in skeletal muscle cells. A) Inhibition of PGC1α transcription utilizing different concentrations of siRNA including 20, 80 and 180 nm after 24 h of differentiation. $^{**}p < 0.001$ and $^{***}p < 0.0001$ compared to control (n = 5); B) Akt phosphorylation determined by western blotting analysis in control and siRNA PGC1α inhibited cells 24 h after differentiation. The cells were incubated in serum-free medium containing either glucose (5.6 mM) or glucose plus insulin (10,000 μU/mL) for 30 min (n = 3 experiments); C) the rate of oxygen consumption obtained from control and siRNA PGC1α inhibited cells 24 h after differentiation. $^{*}p < 0.05$ compared to its respective control (n = 5).

3.9. Involvement of CREB in the catalase overexpression-induced effect on mitochondrial function in insulin resistant muscle cells

To examine the mechanism behind the positive effect of catalase overexpression on mitochondrial function in insulin resistant muscle cells we determined the phosphorylated level of CREB. This nuclear factor has been found to be an important regulator of PGC1α and consequently of mitochondrial biogenesis [23]. A reduction in the phosphorylated level of CREB in fatty acid treated cells with (~25%) or without (~30%) insulin stimulation was observed. The catalase overexpression raised the CREB phosphorylation level in fatty acid treated cells in the presence of insulin (~18%). However, the magnitude of CREB phosphorylation in fatty acid treated cells overexpressing catalase was lower than in control cells (Fig. 9A).

3.10. The CREB mediated effect on mitochondrial function is regulated by Akt

Insulin increased the CREB phosphorylation level in either control (~25%), control transfected (~8%) and fatty acid treated and transfected cells (~18%). However, in fatty acid treated cells overexpressing catalase, the magnitude of CREB phosphorylation was lower than in control (Fig. 9A). The lack of insulin effect on phosphorylated level of CREB and Akt in fatty acid treated cells suggests a possible association of these proteins. We observed that wortmanin, a known inhibitor of Akt phosphorylation reduced the CREB phosphorylation level (~78%) in muscle cells incubated with insulin. This effect was accompanied by a similar reduction in Akt phosphorylation (~92%) (Fig. 9B). These results were confirmed after transfection of control cells with Akt specific siRNA. The total level of Akt was reduced by 31%, an effect that was observed to reduce the Akt phosphorylated level by 88% (Fig. 9C).

To further examine the connection between CREB and mitochondrial function in muscle cells, we next inhibited the CREB transcription utilizing two different sequences of specific siRNA oligos for CREB. We observed that the CREB inhibition was more efficient when the transfection was performed with both sequences (Fig. 10A). In addition, the results showed that the transcription of oxidative genes including PPARβ and PGC1α were also markedly reduced indicating that CREB exerts an important role on mitochondrial function and fatty acid metabolism in skeletal muscle cells (Fig. 10, panels B and C).

4. Discussion

The major finding of this study was that catalase overexpression prevented insulin resistance in muscle cells chronically exposed to fatty acids by improving mitochondrial function and, consequently, glucose and fatty acid metabolism. Although the mechanism is unknown, the PGC1α transcription was observed to be upregulated in parallel with phosphorylated level of CREB. The ability of CREB to stimulate PGC1α altering mitochondrial function is an adaptive response in skeletal muscle cells associated with regulation of a wide spectrum of metabolic genes described to regulate mitochondrial biogenesis, fatty acid metabolism and energy balance [23,24].

Evidence has accumulated that elevated ROS production decreases mitochondrial function and promotes insulin resistance in skeletal muscle [7,9,25,26]. This affirmation is largely supported by the fact that insulin resistance is associated with elevated intracellular lipid content. However, considering the mitochondria as the major site of intracellular ROS production and their poor respiratory capacity in insulin resistant cells, the concept of elevated ROS production in these cells is intriguing. We observed that the elevated occurrence of oxidative stress in insulin resistant cells decreased the transcription of the mitochondrial biogenesis factor PGC1α, which was further accompanied by a reduced citrate synthase activity indicating that mitochondrial respiration was affected. In fact, the mitochondrial function in these cells was severally reduced as indicated by oxygen consumption and also by the ICAT. Although the mechanism by which palmitic acid increased ROS generation is unknown, the impaired oxygen consumption observed in palmitic acid treated cells might have contributed to elevated ROS generation.

Boveris and Chance [27] reported that ROS production is regulated by mitochondrial membrane potential ($\Delta\psi$) as demonstrated by inhibition of H_2O_2 production in isolated mitochondria oxidizing malate and succinate in the presence of CCCP. In agreement, Lui and Huang [28] reported that the addition of malonate, which leads to reduced

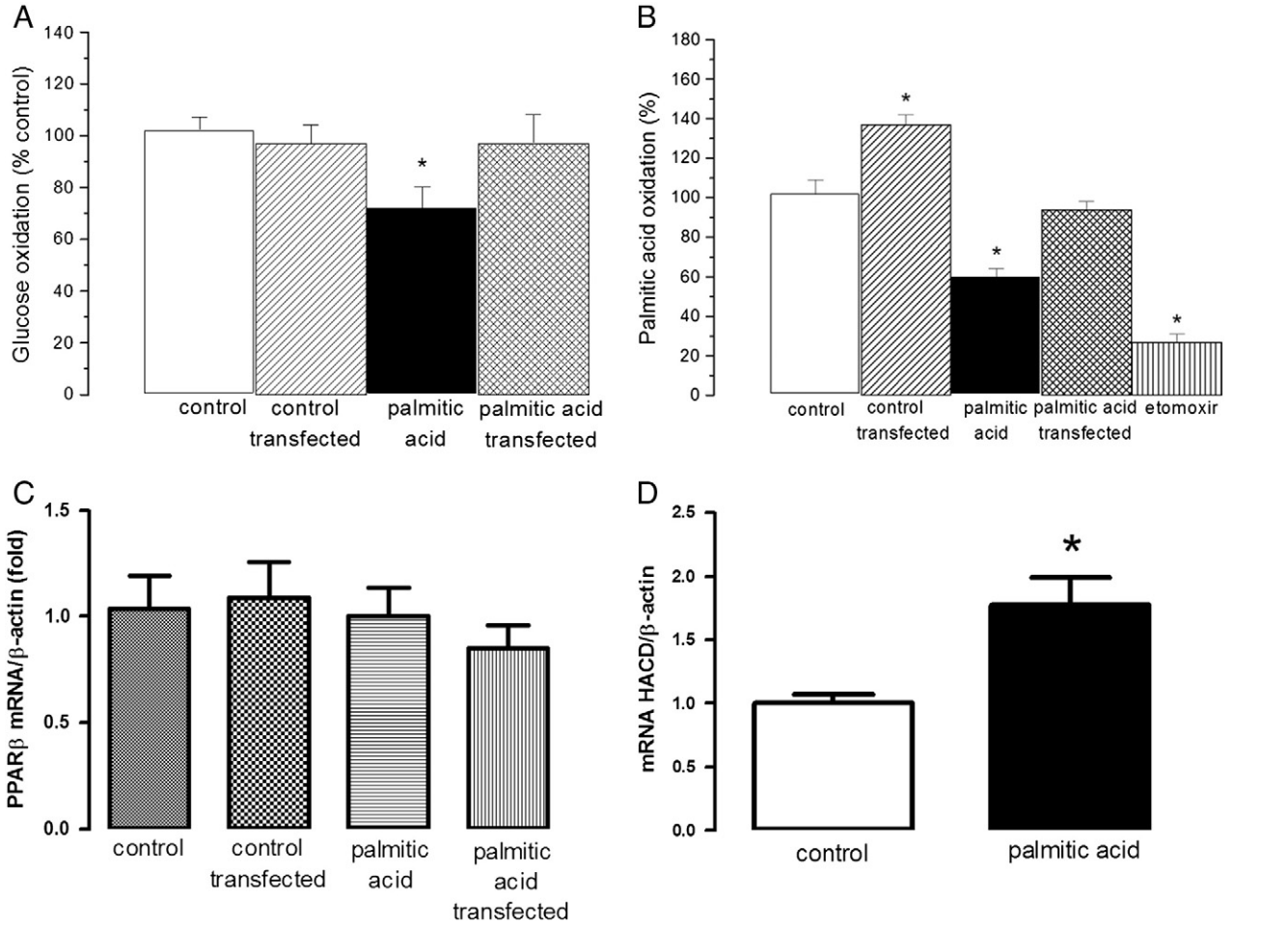

Fig. 8. Metabolism of glucose and fatty acid. A) The results are the mean ± SEM of relative values of glucose oxidation in isolated muscle cells after 24 h of palmitic acid treatment. The cells were incubated during 60 min with serum-free medium containing glucose (5.6 mM) and U-^{14}C-glucose (0.2 μCi/mL). *$p < 0.05$ compared to control ($n = 8–10$); B) Palmitic acid metabolism. Palmitic acid oxidation in isolated muscle cells after 24 h of palmitic acid treatment. The cells were incubated during 60 min with serum-free medium containing glucose (5.6 mM) and [U-^{14}C]-palmitic acid (0.2 μCi/mL). Etomoxir was utilized only as a negative control (vertical line bar). *$p < 0.05$ compared to control ($n = 8–10$); C) The results are mean ± SEM of PPAR-β mRNA at time of 24 h in cultured muscle cells ($n = 5$); D) the results are mean ± SEM of β-hydroxyacyl-CoA-dehydrogenase (β-HACD) mRNA at time of 24 h in cultured muscle cells, *$p < 0.05$ compared to control ($n = 5$).

mitochondrial respiratory state 4 rates, decreases mitochondrial ROS generation indicating that Δψ is closely related to mitochondrial ROS production. Recently, we have observed that mitochondrial uncoupling agent FCCP as well as muscle contractions, two recognized stimuli that reduce the mitochondrial Δψ, markedly increased glucose uptake in insulin resistant muscle cells (data not shown). Thus, the reduced effect of NAC on ROS production was additional evidence that the elevated fatty acid availability changes the mitochondrial Δψ in skeletal muscle cells. This effect was accompanied by reduced Akt phosporylation and low glucose uptake in palmitic acid treated cells. This response was reflected in a low rate of glucose oxidation suggesting that insulin resistance may be an appropriate response to excess provision of nutrients to muscle cells [7,9,14]. Hoehn et al. [29] reported that insulin resistance was rapidly abolished upon exposure to agents that act as mitochondrial uncoupling and SOD mimetics. In contrast, stimulation of ROS production using antimycin A decreased the insulin response in muscle and adipose cells suggesting that the mechanism of insulin resistance protects these cells against oxidative stress imposed by mitochondrial overload.

The oxidation of fatty acid involving the electron transfer by flavoprotein quinone oxidoreductase (ETF-QOR) was observed to increase the rate of ROS production [30–32]. In our experiments, etomoxir decreased hydrogen peroxide production indicating that β-oxidation of fatty acids in cells exhibiting poor mitochondrial activity might exert a central role in mitochondrial ROS production. Despite the pronounced effect of β-oxidation of fatty acids on ROS production, we observed a reduced rate of fatty acid oxidation in insulin resistant cells. However, we did not see any effect on PPARβ transcription level.

In palmitic acid treated cells, the addition of rotenone to permeabilized cells consuming substrates of complex I (malate/glutamate) and II (succinate) decreased the ROS production indicating that reverse electron flow was stimulated, thus favoring ROS production at complex I. Although the mechanism behind this process is unknown, this finding gives evidence that reverse electron flow might be involved with elevated ROS production in insulin resistant cells. In a recent experiment, we observed that the oxygen consumption in isolated muscle cells stimulated by malate/glutamate markedly reduced the rate of ROS production compared to the same condition in the presence of succinate (data not shown). Thus, the elevated transcription of hydrocyacyl-CoA-dehydrogenase, the major site of regulation of β-oxidation, in fatty acid treated cells, might have contributed to an elevated CoQ reduced level [30]. In fact, the low mitochondrial capacity, as indicated by tricarboxylic acid cycle activity, combined to the reduced ratio of mitochondrial substrate to complex I/II ($NADH/FADH_2$) produced by β-oxidation of fatty acids promoted elevated rate of ROS production.

In addition, the fatty acid-induced insulin resistance was demonstrated to reduce the transcription of the antioxidant system

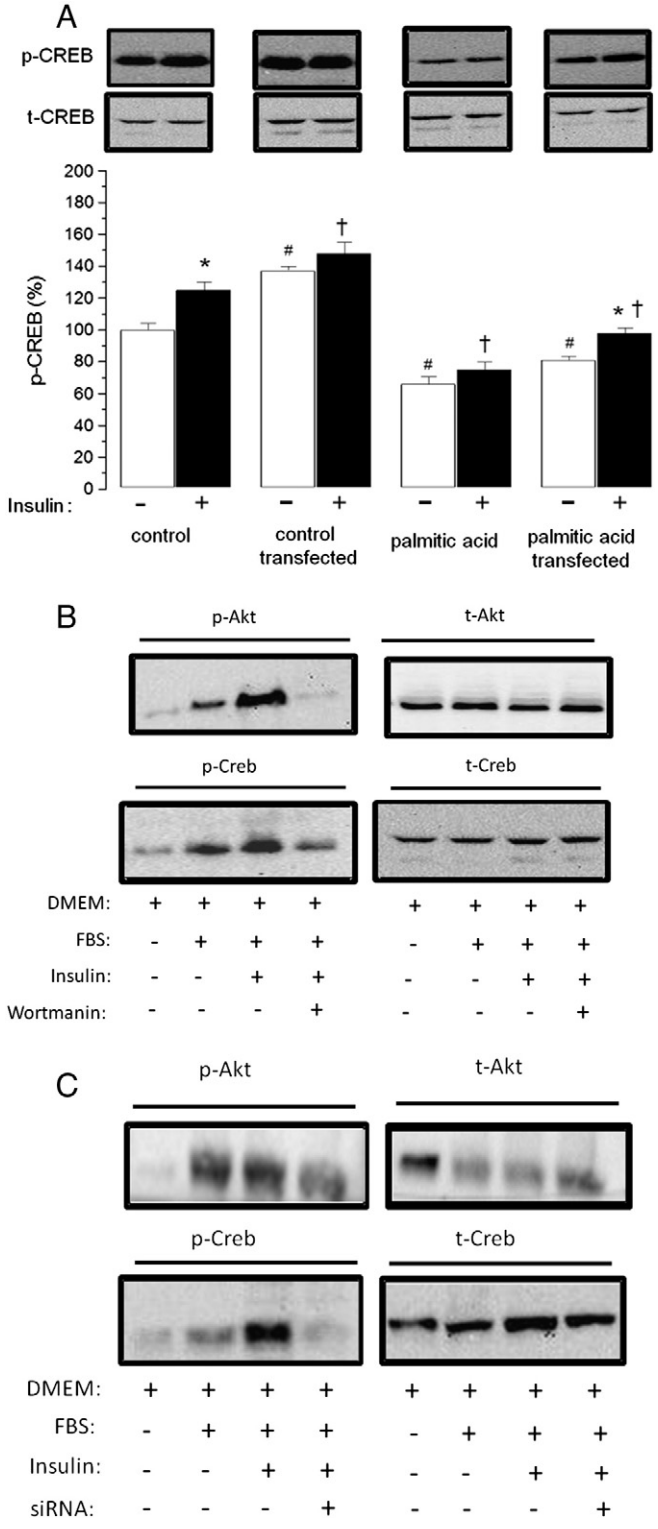

Fig. 9. CREB phosphorylation: A) the results are the mean ± SEM of densitometric analyses from total and phosphorylated level of CREB determined by western blotting. After catalase transfection the muscle cells were exposed to 24 h of palmitic acid treatment and further incubated during 25 min with (black bars) or without (white bars) insulin (10,000 μU). *$p < 0.05$ compared to its respective control; #$p < 0.05$ compared to non-transfected control group without insulin ($n = 5$ experiments); †$p < 0.05$ compared to non-transfected control group with insulin; B) effect of Akt phosphorylation inhibitor, wortmanin (5 μM) on total and phosphorylated level of CREB determined by western blotting in muscle cells incubated with or without insulin. The serum-free medium was used as a negative control, whereas medium containing fetal bovine serum (FBS) was used as a positive control ($n = 5$ experiments) and C) effect of total Akt inhibition using siRNA (20 nM) on total and phosphorylated level of CREB determined by western blotting in muscle cells incubated with or without insulin ($n = 5$ experiments).

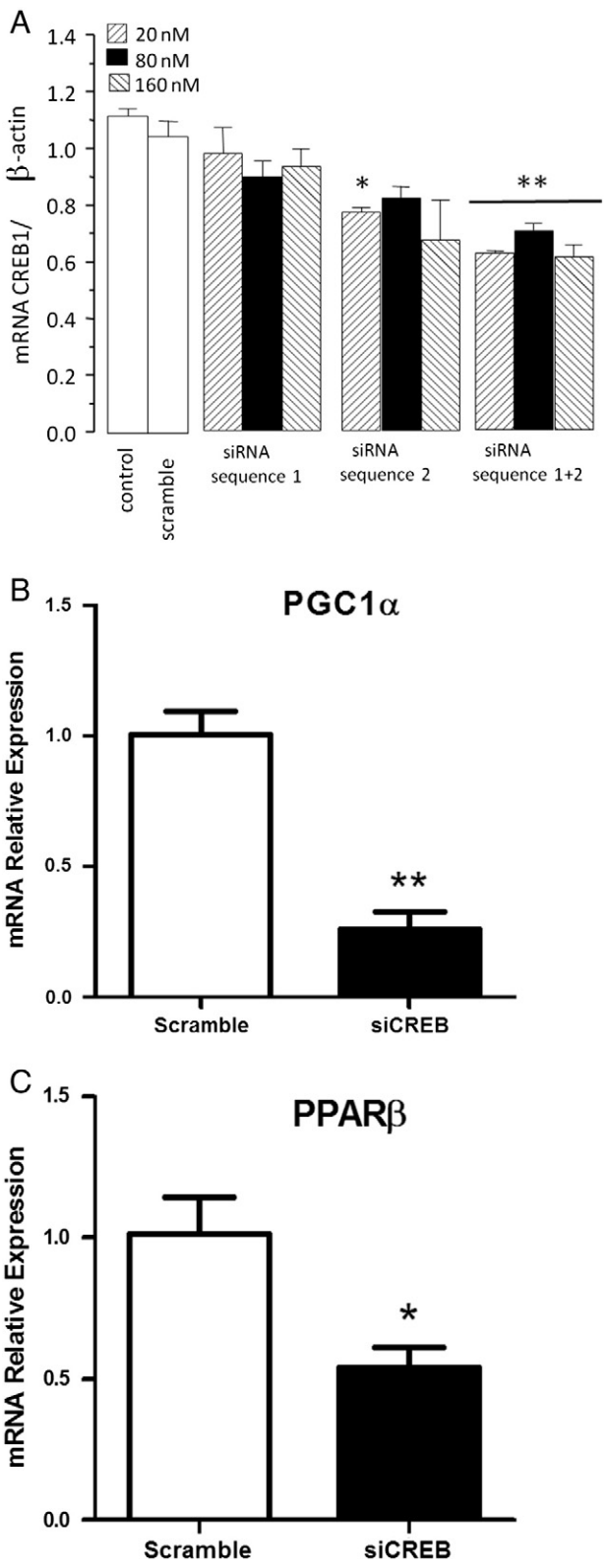

Fig. 10. Effect of CREB inhibition on PGC1α and PPARβ transcription. A) Inhibition of CREB transcription utilizing different concentrations of siRNA including 20, 80 and 160 nm after 24 h of differentiation. The cells were transfected with one or two different sequences of specific siRNA oligos for CREB (sequences 1 and 2). *$p < 0.05$ and **$p < 0.001$ compared to control ($n = 5$); B) effect of CREB inhibition utilizing 20 nm of siRNA 1 and 2 on PGC1α transcription. **$p < 0.001$ compared to scramble ($n = 5$); C) effect of CREB inhibition utilizing 20 nm of siRNA 1 and 2 on PPARβ transcription. *$p < 0.05$ compared to scramble ($n = 5$).

including glutathione peroxidade. This effect must have also contributed to elevated production of ROS observed in these cells. As indicated by the control experiment, the inhibition of catalase expression increased the H_2O_2 production.

However, the overexpression of catalase in palmitic acid treated cells increased the insulin response as reflected by elevated phosphorylated Akt and glucose uptake. The effect of catalase was further confirmed, while catalase overexpression protected the fatty acid treated cells from insulin resistance, inhibition of catalase expression reduced the insulin response. Interestingly, the induction of catalase overexpression in palmitic acid treated cells re-established the transcription level of antioxidant enzymes to the same level as the control, an effect that was also observed to occur in parallel with the increase in citrate synthase activity. In accordance, St-Pierre et al. [33], using siRNA to inhibit PGC1α transcription in neuronal cells, observed a marked reduction in mRNA levels of SOD, catalase, glutatione peroxidade and UCP. In contrast, overexpression of PGC1α abolished this effect improving the transcriptional level of these genes and also demonstrating a coordinated mechanism of control between PGC1α and transcription of antioxidant system. Moreover, the inhibition of catalase expression using siRNA decreased the PGC1α transcription in both control and palmitic acid treated cells. These findings strongly suggest that PGC1α transcription is regulated by the intracellular redox balance indicating that under chronic oxidative stress this transcription factor is downregulated leading to a reduced transcription of intracellular antioxidant enzymes.

The catalase overexpression was also able to attenuate the palmitic acid effect on mitochondrial function as demonstrated by improved oxygen consumption and elevated content of ICAT. However, the oxygen consumption in these cells was lower compared to control. In agreement, Koves et al. [7] observed that in insulin resistant muscle the level of several ICATs was depressed, whereas prevention of insulin resistance by manipulation that restricted fatty acid uptake into mitochondria increased mitochondrial function and ICAT levels. The mechanism by which catalase improved the mitochondria respiration in insulin resistant cells is unknown. However, when the catalase expression was inhibited using siRNA, we observed a diminished mitochondrial respiration, indicating that the intracellular level of catalase was closely related to oxygen consumption in both control and fatty acid treated cells. Similarly, Anderson et al. [9] reported that by attenuating mitochondrial H_2O_2 production, either by using a mitochondrial-target antioxidant or overexpressing catalase, they were able to completely prevent insulin resistance in skeletal muscle of mice submitted to a high-fat diet.

In fact, the excess of intracellular lipid content in skeletal muscle cells has been directly associated with the mechanism of insulin resistance. Under this condition, fatty acids decrease the mitochondrial biogenesis as indicated by reduced transcription of oxidative genes, which are reported to be coordinated by PGC1α, including ATP synthase and mitochondrial uncoupling UCP3 [33,34]. Although the mechanism by which fatty acid reduced the mitochondrial respiration in our study is not completely understood, the reduction in the transcription of oxidative genes might have contributed to lower energy demand in fatty acid treated cells as indicated by the low rate of oxygen consumption in these cells.

The induction in catalase expression prevented the insulin resistance in skeletal muscle cells by a mechanism associated with PGC1α transcription. The transcription of this coactivator has been demonstrated to stimulate mitochondrial biogenesis via activation of nuclear respiratory factors associated with mitochondrial biogenesis and fatty acid metabolism [18,24].

Michael et al. [35] demonstrated in C2C12 and L6 cells through adenovirus-mediated expression of PGC1α that these cells markedly increased the Glut-4 transport transcription, an effect that was correlated with a 3-fold increase in glucose transport in the presence of insulin. Similarly, this effect was also confirmed in transgenic mice overexpressing PGC1α [36]. Transgenic MCK-PGC-1α animals had preserved mitochondrial function and muscle integrity resulting in significantly improved whole-body health. Importantly, MCK-PGC-1α animals also showed improved metabolic responses as evident by increased insulin sensitivity and insulin signaling in aged mice [36]. In addition, we demonstrated now that the inhibition of PGC1α through siRNA technique reduced the phosphorylated level of Akt by approximately 70%, indicating that the PGC1α expression is directly related to insulin response in skeletal muscle cells. Under these conditions, the PGC1α transcription was substantially downregulated leading to reduced mitochondrial respiration. We have, therefore, demonstrated evidence that the mechanism of insulin resistance in skeletal muscle is regulated, at least in part, by mitochondrial function via PGC1α.

The nuclear factor CREB is an important regulator of PGC1α transcription and consequently of mitochondrial biogenesis [23]. This nuclear factor was originally described as a target for PKA-mediated phosphorylation. However, a family of protein kinases has also been involved in CREB phosphorylation including Akt (PKB) [37]. Although the mechanism of control of this process is unknown, the lack of insulin effect on phosphorylated level of both CREB and Akt in palmitic acid treated cells suggests a possible interaction of these proteins. We found that either wortmanin or Akt specific siRNA reduced the CREB phosphorylation level in the presence of insulin suggesting that the reduced Akt phosphorylation observed in palmitic acid treated cells contributed to reduced CREB activation. In myotubes, the expression of TORC, a coactivator of CREB, induced the transcription of PGC1α and consequently the mitochondrial function [38]. In addition, Du and Montminy [35] reported that Akt/PKB promotes cell survival by stimulating the expression of genes via CREB nuclear transduction pathway. However, the induction of catalase expression in both control and palmitic acid treated cells increased the phosphorylated level of CREB. These findings suggest, therefore, that the nuclear transcription factor CREB is an important target for protein kinase B (Akt) during mitochondrial biogenesis and that hydrogen peroxide exerts a central role in this process.

This study supports the hypothesis that an elevated fatty acid supply to mitochondria promotes insulin resistance by a mechanism associated with augmented ROS production through elevated β-oxidation of fatty acids. In addition, we found that induction of catalase expression protected these cells from fatty acid-induced insulin resistance. The improvement in insulin resistance as reflected by reduced Akt phosphorylation was closely related to CREB phosphorylated levels. These effects were observed to increase the transcription of PGC1α and mitochondrial respiration indicating that therapies targeted to reduce intracellular oxidative stress may prevent insulin resistance in skeletal muscle cells exposed to excess of fatty acids.

Acknowledgments

The authors thank Maria Antonieta R Garófaro, Neusa Maria Zanon and Elza Aparecida Filippin for excellent technical assistance. The authors thank Dr. Kleber de Souza for supplying the pcDNA3 plasmid. This work was supported by grants from *Fundação de Amparo à Pesquisa do estado de São Paulo* — FAPESP and *Conselho Nacional de Desenvolvimento Científico e Tecnológico* — CNPq.

Appendix A. Supplementary data

Supplementary data to this article can be found online at http://dx.doi.org/10.1016/j.bbadis.2013.04.029.

References

[1] P.J. Randle, The glucose fatty-acid cycle. Its role in insulin sensitivity and the metabolic disturbances of diabetes mellitus, Lancet 13 (1963) 785–789.
[2] K.F. Petersen, D. Befroy, S. Dufour, J. Dziura, C. Ariyan, D.L. Rothman, L. DiPietro, G.W. Cline, G.I. Shulman, Mitochondrial dysfunction in the elderly: possible role in insulin resistance, Science 300 (2003) 1140–1152.

[3] V.T. Samuel, K.F. Petersen, G.I. Shulman, Lipid-induced insulin resistance: unravelling the mechanism, Lancet 375 (2010) 2267–2277.
[4] D.B. Savage, K.F. Petersen, G.I. Shulman, Disordered lipid metabolism and the pathogenesis of insulin resistance, Physiol. Rev. 87 (2007) 507–520.
[5] M.A. Sabin, C.E. Stewart, E.C. Crowne, S.J. Turner, L.P. Hunt, G.I. Welsh, M.J. Grohmann, J.M. Holly, J.P. Shield, Fatty acid-induced defects in insulin signalling, in myotubes derived from children, are related to ceramide production from almitate rather than the accumulation of intramyocellular lipid, J. Cell. Physiol. 211 (2007) 244–252.
[6] S.M. Hirabara, L.R. Silveira, F. Abdulkader, C.R. Carvalho, J. Procopio, R. Curi, Time-dependent effects of fatty acids on skeletal muscle metabolism, J. Cell. Physiol. 210 (2007) 7–15.
[7] T.R. Koves, J.R. Ussher, R.C. Noland, D. Slentz, M. Mosedale, O. Ilkayeva, J. Bain, R. Stevens, J.R. Dyck, C.B. Newgard, G.D. Lopaschuk, D.M. Muoio, Mitochondrial overload and incomplete fatty acid oxidation contribute to skeletal muscle insulin resistance, Cell. Metab. 7 (2008) 45–56.
[8] C.S. Choi, D.B. Savage, L. Abu-Elheiga, Z.X. Liu, S. Kim, A. Kulkarni, A. Distefano, Y.J. Hwang, R.M. Reznick, R. Codella, D. Zhang, G.W. Cline, S.J. Wakil, G.I. Shulman, Continuous fat oxidation in acetyl-CoA carboxylase 2 knockout mice increases total energy expenditure, reduces fat mass, and improves insulin sensitivity, Proc. Natl. Acad. Sci. U.S.A. 104 (2007) 16480–16485.
[9] E.J. Anderson, M.E. Lustig, K.E. Boyle, T.L. Woodlief, D.A. Kane, C.T. Lin, J.W. Price, L. Kang, P.S. Rabinovitch, H.H. Szeto, J.A. Houmard, R.N. Cortright, D.H. Wasserman, P.D. Neufer, Mitochondrial H_2O_2 emission and cellular redox state link excess fat intake to insulin resistance in both rodents and humans, J. Clin. Invest. 119 (2009) 573–581.
[10] L.J. van Loon, B.H. Goodpaster, Increased intramuscular lipid storage in the insulin-resistant and endurance-trained state, Pflugers Arch. 451 (2006) 606–616.
[11] L.R. Silveira, J. Fiamoncini, S.M. Hirabara, J. Procópio, T.D. Cambiaghi, C.H. Pinheiro, L.R. Lopes, R. Curi, Updating the effects of fatty acids on skeletal muscle, J. Cell. Physiol. 217 (2008) 1–12.
[12] K. Loh, H. Deng, A. Fukushima, X. Cai, B. Boivin, S. Galic, C. Bruce, B.J. Shields, B. Skiba, L.M. Ooms, N. Stepto, B. Wu, C.A. Mitchell, N.K. Tonks, M.J. Watt, M.A. Febbraio, P.J. Crack, S. Andrikopoulos, T. Tiganis, Reactive oxygen species enhance insulin sensitivity, Cell. Metab. 10 (2009) 260–272.
[13] M. Ristow, K. Zarse, A. Oberbach, N. Klöting, M. Birringer, M. Kiehntopf, M. Stumvoll, C.R. Kahn, M. Blüher, Antioxidants prevent health-promoting effects of physical exercise in humans, Proc. Natl. Acad. Sci. U.S.A. 106 (2009) 8665–8670.
[14] T.R. Koves, P. Li, J. An, T. Akimoto, D. Slentz, O. Ilkayeva, G.L. Dohm, Z. Yan, C.B. Newgard, D.M. Muoio, Peroxisome proliferator-activated receptor-gamma co-activator 1alpha-mediated metabolic remodeling of skeletal myocytes mimics exercise training and reverses lipid-induced mitochondrial inefficiency, J. Biol. Chem. 280 (2005) 33588–33598.
[15] J. Lynge, C. Juel, Y. Hellsten, Extracellular formation and uptake of adenosine during skeletal muscle contraction in the rat: role of adenosine transporters, J. Physiol. 537 (2001) 597–605.
[16] P.P. Hommelberg, R.C. Langen, A.M. Schols, Fatty acid-induced NF-kB activation and insulin resistance in skeletal muscle are chain length dependent, Am. J. Physiol. Endocrinol. Metab. 296 (2009) 114–120.
[17] P.A. Srere, H. Brazil, L. Gonen, The citrate condensing enzyme of pigeon breast muscle and moth flight muscle, Acta Chem. Scand. 17 (1963) 129–134.
[18] Z. Wu, P. Puigserver, U. Andersson, C. Zhang, G. Adelmant, V. Mootha, A. Troy, S. Cinti, B. Lowell, R.C. Scarpulla, B.M., Mechanisms controlling mitochondrial biogenesis and respiration through the thermogenic coactivator PGC-1, Cell 98 (1999) 115–124.
[19] S.M. Hirabara, L.R. Silveira, L.C. Alberici, C.V. Leandro, R.H. Lambertucci, G.C. Polimeno, M.F. Cury Boaventura, J. Procopio, A.E. Vercesi, R. Curi, Acute effect of fatty acids on metabolism and mitochondrial coupling in skeletal muscle, Biochim. Biophys. Acta 1757 (2006) 57–66.
[20] S.M. Hirabara, C.R. Oliveira Carvalho, J.R. Mendonça, E. Piltcher Haber, L.C. Fernandes, R. Curi, Palmitate acutely raises glycogen synthesis in rat soleus muscle by a mechanism that requires its metabolization (Randle cycle), FEBS Lett. 541 (2003) 109–114.
[21] P. Seale, H.M. Conroe, J. Estall, S. Kajimura, A. Frontini, J. Ishibashi, P. Cohen, S. Cinti, B.M. Spiegelman, Prdm16 determines the thermogenic program of subcutaneous white adipose tissue in mice, J. Clin. Invest. 121 (2011) 96–105.
[22] H.U. Bergmeyer, Methods of Enzymatic Analysis, second edition, Academic Press, New York (NY), 1974.
[23] P. Puigserver, B.M. Spiegelman, Peroxisome proliferator–activated receptor–gamma coactivator 1 alpha (PGC-1 alpha): transcriptional coactivator and metabolic regulator, Endocr. Rev. 24 (2011) 78–90.
[24] P. Puigserver, Z. Wu, C.W. Park, R. Graves, M. Wright, B.M. Spiegelman, A cold-inducible coactivator of nuclear receptors linked to adaptive thermogenesis, Cell 92 (1998) 829–839.
[25] E.R. Ropelle, J.R. Pauli, P.O. Prada, C.T. de Souza, P.K. Picardi, M.C. Faria, D.E. Cintra, M.F. Fernandes, M.B. Flores, L.A. Velloso, M.J. Saad, J.B. Carvalheira, Reversal of diet-induced insulin resistance with a single bout of exercise in the rat: the role of PTP1B and IRS-1 serine phosphorylation, J. Physiol. 577 (2006) 997–1007.
[26] C.H.J. Pinheiro, L.R. Silveira, R.T. Nachbar, K.F. Vitzel, R. Curi, Regulation of glycolysis and expression of glucose metabolism-related genes by reactive oxygen species in contracting skeletal muscle cells, Free Radic. Biol. Med. 48 (2010) 953–960.
[27] A. Boveris, B. Chance, The mitochondrial generation of hydrogen peroxide. General properties and effect of hyperbaric oxygen, Biochem. J. 134 (1973) 707–716.
[28] S.S. Liu, Generating, partitioning, targeting and functioning of superoxide in mitochondria, Biosci. Rep. 17 (1997) 259–272.
[29] K.L. Hoehn, A.B. Salmon, C. Hohnen-Behrens, N. Turner, A.J. Hoy, G.J. Maghzal, R. Stocker, H. Van Remmen, E.W. Kraegen, G.J. Cooney, A.R. Richardson, D.E. James, Insulin resistance is a cellular antioxidant defense mechanism, Proc. Natl. Acad. Sci. U.S.A. 106 (2009) 17787–17792.
[30] A. Boveris, N. Oshino, B. Chance, The cellular production of hydrogen peroxide, Biochem. J. 128 (1972) 617–630.
[31] J. St-Pierre, J.A. Buckingham, S.J. Roebuck, M.D. Brand, Topology of superoxide production from different sites in the mitochondrial electron transport chain, J. Biol. Chem. 277 (2002) 44784–44790.
[32] K.H. Fisher-Wellman, P.D. Neufer, Linking mitochondrial bioenergetics to insulin resistance via redox biology, Trends Endocrinol. Metab. 23 (2012) 142–153.
[33] J. St-Pierre, S. Drori, M. Uldry, J.M. Silvaggi, J. Rhee, S. Jäger, C. Handschin, K. Zheng, J. Lin, W. Yang, D.K. Simon, R. Bachoo, B.M. Spiegelman, Suppression of reactive oxygen species and neurodegeneration by the PGC-1 transcriptional coactivators, Cell 127 (2006) 397–408.
[34] D.E. Befroy, K.F. Petersen, S. Dufour, G.F. Mason, D.L. Rothman, G.I. Shulman, Increased substrate oxidation and mitochondrial uncoupling in skeletal muscle of endurance-trained individuals, Proc. Natl. Acad. Sci. U.S.A. 105 (2008) 16701–16706.
[35] L.F. Michael, Z. Wu, R.B. Cheatham, P. Puigserver, G. Adelmant, J.J. Lehman, D.P. Kelly, B.M. Spiegelman, Restoration of insulin-sensitive glucose transporter (GLUT4) gene expression in muscle cells by the transcriptional coactivator PGC-1, Proc. Natl. Acad. Sci. U.S.A. 98 (2001) 3820–3825.
[36] T. Wenz, S.G. Rossi, R.L. Rotundo, B.M. Spiegelman, C.T. Moraes, Increased muscle PGC-1alpha expression protects from sarcopenia and metabolic disease during aging, Proc. Natl. Acad. Sci. U.S.A. 106 (2009) 20405–20410.
[37] K. Du, M. Montminy, CREB is a regulatory target for the protein kinase Akt/PKB, J. Biol. Chem. 273 (1998) 32377–32399.
[38] Z. Wu, X. Huang, Y. Feng, C. Handschin, Y. Feng, P.S. Gullicksen, O. Bare, M. Labow, B.M. Spiegelman, S.C. Stevenson, Transducer of regulated CREB-binding proteins (TORCs) induce PGC-1alpha transcription and mitochondrial biogenesis in muscle cells, Proc. Natl. Acad. Sci. U.S.A. 103 (2006) 14379–14384.